

Comparison and Bayesian Estimation of Feature Allocations

David B. Dahl

Department of Statistics, Brigham Young University

Devin J. Johnson

Department of Statistical Science, Duke University

R. Jacob Andros

Department of Statistics, Brigham Young University

July 29, 2022

Abstract

Feature allocation models postulate a sampling distribution whose parameters are derived from shared features. Bayesian models place a prior distribution on the feature allocation, and Markov chain Monte Carlo is typically used for model fitting, which results in thousands of feature allocations sampled from the posterior distribution. Based on these samples, we propose a method to provide a point estimate of a latent feature allocation. First, we introduce FARO loss, a function between feature allocations which satisfies quasi-metric properties and allows for comparing feature allocations with differing numbers of features. The loss involves finding the optimal feature ordering among all possible, but computational feasibility is achieved by framing this task as a linear assignment problem. We also introduce the FANGS algorithm to obtain a Bayes estimate by minimizing the Monte Carlo estimate of the posterior expected FARO loss using the available samples. FANGS can produce an estimate other than those visited in the Markov chain. We provide an investigation of existing methods and our proposed methods. Our loss function and search algorithm are implemented in the `fangs` package in R.

Keywords: Bayesian nonparametrics, Indian buffet process, linear assignment problem, Hamming distance.

1 Introduction

Bayesian data analysis consists of two major tasks: sampling from the posterior distribution (either directly or through some approximation), and then summarizing those posterior draws in a way that is relevant to the problem at hand. Parameter estimation is often a straightforward process, with the posterior mean, median, mode, or a credible interval being sufficient in many cases. However, for more complex parameters not contained in \mathbb{R}^n , a different approach is necessary.

Feature allocation models from Bayesian nonparametrics are an example of such a case where a more tailored estimation approach is needed. A feature allocation $\rho = \{S_1, \dots, S_K\}$ is a multiset of subsets (i.e., features) such that each subset $S_k \subseteq \{1, \dots, n\}$ is nonempty. Being a multiset, the order of the subsets is irrelevant, and there may be duplicates. In contrast to partitions, these subsets are not necessarily mutually exclusive nor exhaustive. For some subset $S_k \in \rho$, we say that item i has feature k if $i \in S_k$, and items i and j share feature k if $i \in S_k$ and $j \in S_k$. In model construction, features are often used to arrange data y_1, \dots, y_n such that data sharing a feature k have some aspect of the data model in common. A feature allocation ρ can alternatively be represented by a binary matrix Z , with n rows and K columns, containing 1 in the (i, j) element if and only if $i \in S_k$, for $k = 1, \dots, K$. Griffiths and Ghahramani (2011) defined an equivalence class for these binary feature allocation matrices based on a left-ordering function $lof(\cdot)$, which reorders the columns of a feature allocation matrix from left to right by the binary number of each column in descending order. Under this equivalence class, the order of subsets in ρ is irrelevant; likewise, the order of the columns (or features) in Z is not important. Furthermore, under the left-ordering function, a column of all zeros represents a null column (or an empty feature), so adding a column of zeros to Z does not change its equivalence.

Feature allocations have been used for a wide range of applications, most frequently in biostatistics. Such applications include disease classification (Warr et al., 2021), cell subpopulation identification (Lui et al., 2021), tumor heterogeneity inference (Xu et al., 2015), and symptom-disease relationship modeling (Ni et al., 2020b). These same studies have also explored methods for sampling feature allocations using MCMC. But again,

while obtaining posterior samples is crucial, it is only part of the inference problem. We propose the FARO loss function and FANGS search algorithm that work in tandem to provide a feature allocation point estimate using the posterior samples. FARO loss is not restricted to comparing matrices with a common number of features and does not discriminate based on feature ordering. The proposed FANGS search algorithm can then quickly and repeatedly compute Monte Carlo estimates of the expected FARO loss for different candidate estimates. It uses these candidates to optimize the feature allocation space and will almost certainly find a better feature allocation than those visited by the Markov chain. Our loss function and search algorithm are implemented in the `fangs` package for R.

The paper proceeds as follows. In Section 2, we provide additional background on feature allocations and review the existing literature. In Section 3, we detail a new loss function and the unique advantages that it holds over the previous losses described in Section 2. In Section 4, we explain the intuition behind our FANGS search algorithm that works in tandem with the FARO loss function proposed in Section 3. Section 5 contains a comparison through simulation studies of the existing search algorithms with our proposed FANGS method. Finally, Section 6 provides a summary of the contributions these methods make to the literature on Bayesian feature allocation models.

2 Existing Literature on Feature Allocations

In this section, we review existing loss function for feature allocations and existing search algorithms for feature allocation estimation. This provides a context for our proposed FARO loss function (in Section 3) and FANGS search algorithm (in Section 4).

2.1 Background on Loss Functions

In Bayesian statistics, we typically choose a loss function that can measure the distance between two objects in the parameter space (e.g., an estimator $\hat{\theta}$ and the true parameter value θ). A higher loss indicates more dissimilarity between the estimator and the pa-

parameter value. Then, the posterior expectation of that loss function is minimized to find the Bayesian estimator of the parameter. In the case of feature allocations, for some loss function $L(\rho, \hat{\rho})$ used to measure the loss in estimating ρ with $\hat{\rho}$, the Bayes estimate $\hat{\rho}^*$ is:

$$\hat{\rho}^* = \underset{\hat{\rho}}{\operatorname{argmin}} \mathbb{E}(L(\rho, \hat{\rho}) \mid \mathcal{D}) \quad \text{or} \quad \hat{Z}^* = \underset{\hat{Z}}{\operatorname{argmin}} \mathbb{E}(L(Z, \hat{Z}) \mid \mathcal{D}), \quad (1)$$

where \mathcal{D} is the observed data, and \hat{Z}^* and $L(Z, \hat{Z})$ are parameterized in binary matrix notation and are equivalent to $\hat{\rho}^*$ and $L(\rho, \hat{\rho})$. Without loss of generality, we assume that if the estimator (i.e., $\hat{\rho}$ or \hat{Z}) is equal to the true parameter (i.e., ρ or Z), then the loss function evaluates to zero. Otherwise, the loss evaluates to a positive value that represents the “cost” associated with using the chosen estimator instead of the truth. In most applications, the posterior expectation in (1) is approximated using posterior samples:

$$\mathbb{E}(L(\rho, \hat{\rho}) \mid \mathcal{D}) \approx \frac{1}{B} \sum_{b=1}^B L(\rho_b, \hat{\rho}) \quad \text{or} \quad \mathbb{E}(L(Z, \hat{Z}) \mid \mathcal{D}) \approx \frac{1}{B} \sum_{b=1}^B L(Z_b, \hat{Z}), \quad (2)$$

where ρ_1, \dots, ρ_B or Z_1, \dots, Z_B are B feature allocation samples from a posterior distribution $p(\rho \mid \mathcal{D})$ or $p(Z \mid \mathcal{D})$. Samples are often obtained through considerable effort from several MCMC chains; we simply assume they are available. We seek to find an estimate using the available samples that summarizes the feature allocation distribution.

2.2 Existing Loss Functions for Feature Allocations

Loss functions for estimating parameters contained in \mathbb{R}^n — such as squared error loss or absolute error loss — are well studied and frequently applied. In this subsection, we review the relatively modest literature on loss functions for feature allocations.

2.2.1 Zero-One Loss

[Gershman et al. \(2015\)](#) proposed using the maximum a posteriori (MAP) feature allocation in the context of the distance dependent Indian Buffet Process (ddIBP). [Warr et al. \(2021\)](#) successfully implemented this method in a classification study of Alzheimer’s disease neuroimaging. [Xu et al. \(2015\)](#) devised an objective function, similar to a penalized likelihood function, to find the MAP. Recall that the MAP estimator, in theory, relies on the zero-

one loss function. When using the MAP estimator in feature allocation summarization, we are required to have either: i) access to a computable posterior density that can be optimized, or ii) enough posterior samples and small enough matrix dimensions that the same feature allocation Z has been visited multiple times in the Markov chain. The first requirement may be tedious since a set of posterior samples would not be enough to carry out estimation, and the second is unlikely to be met in nontrivial applications. Finally, the MAP estimate may not well represent the “center” of the posterior feature allocation distribution, and could be problematic in multimodal or heavily skewed distributions.

2.2.2 Loss Based on Pairwise Similarity

Lui et al. (2021) modeled cytometry data using a latent feature allocation model and based their loss function on the pairwise similarity matrix (PSM), denoted by Ψ . The (i, j) element of Ψ gives the expected number of features shared by items i and j . The PSM Ψ is estimated from posterior samples Z_1, \dots, Z_B as $\hat{\Psi}_{ij} = \frac{1}{B} \sum_{b=1}^B Z_b Z'_b$, where Z' is the transpose of Z and the summation is elementwise. Lui et al. (2021) proposed a feature allocation estimate \hat{Z} which minimizes the sum of squared distances from each element of Ψ :

$$\hat{Z} = \underset{Z}{\operatorname{argmin}} \sum_{i=1}^n \sum_{j=1}^n ((ZZ')_{ij} - \Psi_{ij})^2. \quad (3)$$

This approach mirrors the literature of partition estimation from Dahl (2006) in which the sum of squares to a clustering adjacency matrix was minimized. Lau and Green (2007) proposed minimizing the posterior expectation of the popular Binder loss. Later, Dahl and Newton (2007) showed that the least-squares estimate of a partition is actually equivalent to minimizing Binder loss. A key to this equivalence relies on the fact that a partition is unique to its adjacency matrix. Unfortunately, a feature allocation Z is not always unique to its adjacency matrix ZZ' , as demonstrated in Figure 1. Two distinct feature allocations are shown here, one with three features and one with four features. Upon inspection, these two feature allocations seem to be quite distinct, and yet they still map to the same adjacency matrix. Hence, a loss function using the adjacency matrix would not distinguish between these two feature allocations. This problem is amplified as n and K increase.

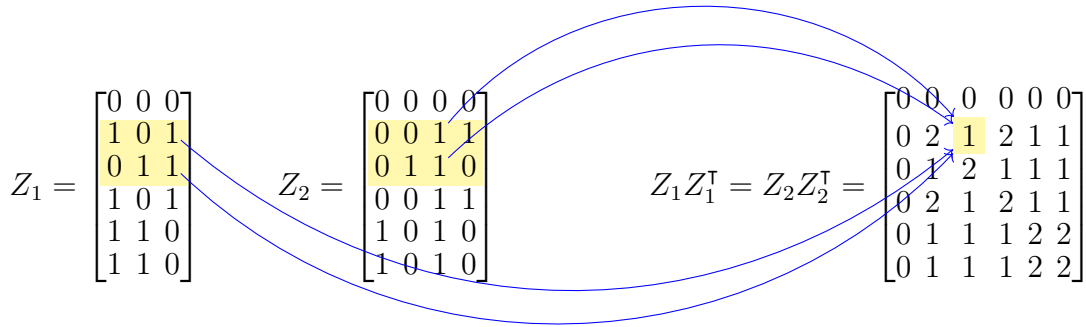


Figure 1: The distinct feature allocations Z_1 and Z_2 map to the same adjacency matrix.

2.2.3 Hamming Distance

Ni et al. (2020b) proposed a double feature allocation (DFA) model for patient-disease data. They used a loss function conditioned on \hat{K} , the modal number of features from the samples. The distance between a given binary matrix $Z \in \{0, 1\}^{n \times \hat{K}}$ and an estimate \hat{Z} was defined as the minimum Hamming distance between Z and the set of all column permutations of \hat{Z} , which they denote using $\pi(\hat{Z})$ (Equation 4). The Hamming distance between two matrices Z and \hat{Z} (with the same number of columns) simply counts the number of (i, j) indices that disagree. Note that $\mathbb{I}(Z_{ij} \neq \hat{Z}_{ij})$ is 1 if the (i, j) entries of Z and \hat{Z} disagree, and is 0 if they are the same.

$$\mathcal{H}(Z, \hat{Z}) = \sum_{i=1}^n \sum_{j=1}^K \mathbb{I}(Z_{ij} \neq \hat{Z}_{ij}) \quad L(Z, \hat{Z}) = \min_{\pi} \mathcal{H}(Z, \pi(\hat{Z})) \quad (4)$$

However, their loss function forces the number of features in their estimated feature allocation to match the expected number of features. In practice, any posterior samples whose number of features differ from the observed modal number of features (\hat{K}) are discarded when estimating the feature allocation. In addition, examining all column permutations of a feature allocation matrix gets extremely difficult for high values of K , with order $\mathcal{O}(K!)$. For example, $10!$ is approximately 3.6 million, and examining that many different permutations takes over 6 seconds (see Table 1 in Section 3.4). To find the feature allocation with the lowest expected loss among the B posterior samples, the loss would have to be computed B^2 times, so spending even a few seconds on each column alignment is not viable.

In spite of the computational disadvantages, column-permuted Hamming distance may be the most intuitive of all the losses discussed so far. Binder loss is commonly used for partitions (Dahl et al., 2022) and can be expressed in terms of Hamming distance (Wade

and Ghahramani, 2018). It would then be logical to use the Hamming distance to formulate a loss function for feature allocation estimation, which we explore further in Section 3.

2.3 Existing Search Algorithms for Feature Allocations

As was the case with loss functions for feature allocations, there is only a relatively modest literature on search algorithms for minimizing the posterior expected loss in feature allocation estimation. A loss function without an effective means to minimize its posterior expectation is of little practical use when seeking to find a Bayes estimator.

The studies discussed in the previous section included the simulations from the AIBD paper (Warr et al., 2021), the cytometry data model (Lui et al., 2021), and the DFA model for patient-disease relationships (Ni et al., 2020b). The loss functions in these studies were different; the first used zero-one loss, the second used a sum of squares function on the PSM, and the last used Hamming distance. However, they all used the same search algorithm, namely, the “draws method” (Dahl, 2006). The draws method comprises finding the feature allocation among those sampled that minimizes the estimated expected loss:

$$\hat{Z}^* = \underset{\hat{Z}}{\operatorname{argmin}} \frac{1}{B} \sum_{b=1}^B L(Z_b, \hat{Z}) \text{ for } \hat{Z} \in \{Z_b : b = 1, \dots, B\} \quad (5)$$

In the case of the DFA model, the draws method is restricted to only search among those sampled feature allocations whose number of features equals the modal number of features \hat{K} . That is, rather than selecting from all posterior samples $\hat{Z} \in \{Z_b : b = 1, \dots, B\}$, the algorithm is limited to choosing from $\hat{Z} \in \{Z^{n \times K} : K = \hat{K}\} \subseteq \{Z_b : b = 1, \dots, B\}$.

Though computationally efficient and widely applicable, the draws method is clearly flawed — its chosen estimate is restricted to the samples visited in the Markov chain (Dahl et al., 2022). There almost certainly exists an estimate within the parameter space (but not sampled in the chains) that yields lower loss than the minimizing draw. At the same time, it would be impractical to conduct an exhaustive search over all possible feature allocation matrices; for a given binary $n \times K$ matrix, there exist $2^{n \times K}$ possible objects. Even if $n = 25$ and $K = 4$, this would entail searching through more than 10^{29} matrices.

Besides the draws method, we are aware of one other search algorithm used by Zeng et al.

(2018) in a tumor subclone identification study. They called their method SIFA, short for subclone identification using feature allocations. In the SIFA example, all posterior samples had the same number of features. They sequentially reordered the columns of each sample by finding the column permutation that minimized the Hamming distance between Z_i and Z_{i-1} for $i = 2, \dots, B$. Within these aligned feature allocations, the element-wise mode was computed for all (i, j) entries to form the feature allocation estimate. Their approach computes all possible column reorderings, much like Ni et al. (2020b), and thus becomes infeasible for increasing K . This idea is intriguing as it is not stochastic and can explore more than just the sampled draws, but it comes at a heavy computational expense.

In short, the ideal search algorithm should be computationally efficient for increasing K , more expansive than the draws method, and avoid the cost of an exhaustive search.

3 Feature Allocations Reordered Optimally (FARO)

In this section we introduce FARO (an acronym for **f**eature **a**llocations **r**eordered **o**ptimally) loss as a loss function between two feature allocations. As we explain in this section, our FARO loss is simply the minimum generalized Hamming distance between all column permutations of two feature allocation matrices. Importantly, FARO loss can compare matrices having different numbers of features K . Minimization problems based on computing the expected FARO loss only need access to a set of sampled feature allocations; a closed-form posterior density is not necessary. FARO loss is also more computationally efficient than previous loss functions and can therefore be evaluated repeatedly and rapidly. This will be crucial for the feasibility of our FANGS search algorithm that we introduce in Section 4.

3.1 Relation to Hamming Distance

Binder (1978) loss is a popular loss function for partitions that can be expressed in terms of Hamming distances (Wade and Ghahramani, 2018) between adjacency matrices from partitions. Our FARO loss for feature allocations is also based on Hamming distance, but the Hamming distances are now computed among the binary matrices (e.g., Z) instead of

adjacency matrices (e.g., ZZ'). Using Hamming distance to compare feature allocations is a promising start and is an important component of FARO loss inspired by the existing literature, but FARO loss makes four key additional contributions. First, FARO loss can compare feature allocations with different numbers of features, thus permitting all posterior samples to aid in estimation (Section 3.2). Second, we introduce the use of unequal penalties when computing Hamming distance between feature allocations (Section 3.3), following the flexibility of Binder (1978) loss and generalized variation of information (Dahl et al., 2022) in the partition literature. Our generalization with differential costs induces control over the sparsity when estimating a feature allocation. Third, we note that finding the minimum Hamming distance for all column permutations does not require an exhaustive search. Rather, we formulate this as a linear assignment problem (Section 3.4) which is well-studied in the computer science literature. This formulation allows for rapid computation of FARO loss, opening the possibility of repeated computation of the posterior expected loss in our proposed search algorithm. Fourth, we prove that FARO loss is a quasi-metric in Section 3.5.

3.2 Imbalanced Dimensions

The Hamming distance between Z and \hat{Z} is a weighted sum of disagreements between their corresponding indices and is only defined for matrices with the same dimensions. Ni et al. (2020b) implicitly assign infinite loss for any feature allocation whose number of features K does not equal the modal number of features \hat{K} . Thus any posterior samples with $K \neq \hat{K}$ are completely discarded in their estimation of the feature allocation. In another paper, Ni et al. (2020a) proposed a consensus Monte Carlo (CMC) approach for scaling feature allocations modeling big data where they remove the excess columns from the matrix with more features. In Zeng et al. (2018), the sampling process was such that all feature allocation draws had the exact same number of features, eliminating the need to address the dimensionality problem. Our approach is different from all three of these approaches. FARO loss accounts for an imbalanced number of columns by augmenting the matrix having fewer columns with empty features (i.e., columns of zeros). This does

not alter equivalence under the left-ordering equivalence class (Griffiths and Ghahramani, 2011) and simplifies the comparison between matrices based on Hamming distance.

3.3 Generalized Hamming Distance

In Ni et al. (2020b), Zeng et al. (2018), and in our own discussion to this point, Hamming distance $\mathcal{H}(Z, \hat{Z})$ has been defined as the summation of all disagreements between indices of two feature allocation matrices.

$$\mathcal{H}(Z, \hat{Z}) = \sum_{i=1}^n \sum_{j=1}^K \mathbb{I}(Z_{ij} \neq \hat{Z}_{ij}) = \sum_{i=1}^n \sum_{j=1}^K [\mathbb{I}(Z_{ij} = 1 \cap \hat{Z}_{ij} = 0) + \mathbb{I}(Z_{ij} = 0 \cap \hat{Z}_{ij} = 1)]$$

Implicitly, there is a penalty of 1 when $Z_{ij} \neq \hat{Z}_{ij}$ regardless of whether this disagreement arises from $Z_{ij} = 1$ and $\hat{Z}_{ij} = 0$ or from $Z_{ij} = 0$ and $\hat{Z}_{ij} = 1$. Binder (1978) proposed a partition loss with two distinct penalty parameters a and b . That is, in its equal-cost form, we would have $a = b = 1$. Dahl et al. (2022) showed that differential costs $a \neq b$ allows for tuning of the number of clusters present in a partition estimate. In the same way, we propose that the penalties a and b can be used for feature allocation estimation. Without loss of generality, let $a, b \in (0, 2)$ and $a + b = 2$. We call this function the generalized Hamming distance¹ $\mathcal{H}_G(Z, \hat{Z})$:

$$\mathcal{H}_G(Z, \hat{Z}) = \sum_{i=1}^n \sum_{j=1}^K [a \cdot \mathbb{I}(Z_{ij} = 1 \cap \hat{Z}_{ij} = 0) + b \cdot \mathbb{I}(Z_{ij} = 0 \cap \hat{Z}_{ij} = 1)] \quad (6)$$

Our FARO loss is simply the minimum generalized Hamming distance between all column permutations of two feature allocation matrices. As is the case for controlling the number of clusters in partition estimation (Dahl et al., 2022), the ability to adjust the penalties controls the sparsity in feature allocation estimation. This becomes particularly important when dealing with samples having extremely high K , as they tend to yield less interpretable feature allocation estimates. For the remainder of the paper, we refer to generalized Hamming distance instead of the original Hamming distance.

¹This should not be confused with the definition of generalized Hamming distance given by Bookstein et al. (2002) in the computer science literature to compare bitmaps and bitstrings.

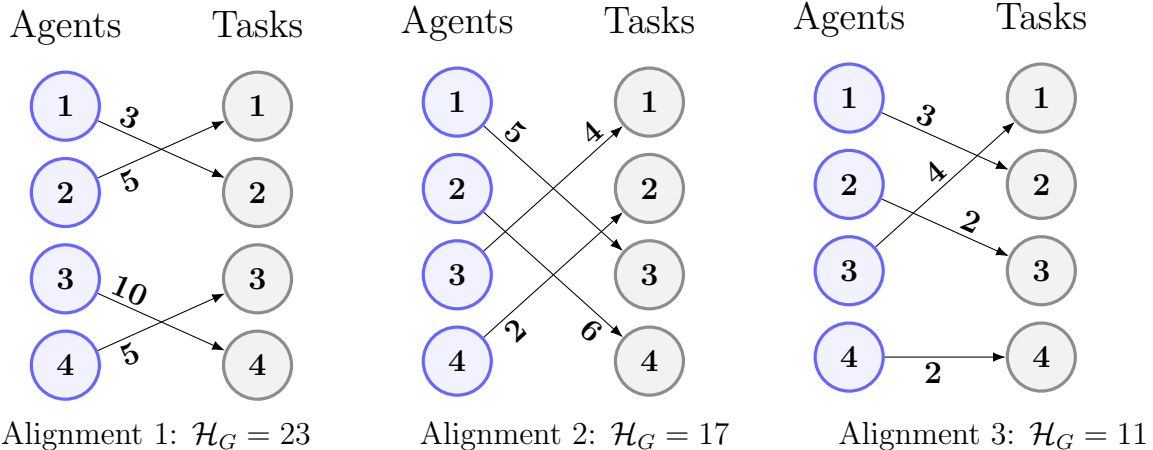


Figure 2: An example of the linear assignment problem in the context of assigning an agent (a column of Z) to a task (a column of \hat{Z}). While the first two alignments (left and middle) lead to costs of 23 and 17, the last alignment yields the optimal cost of 11.

3.4 The Linear Assignment Problem

Even after augmenting a smaller matrix with columns of zeros, the generalized Hamming distance between two matrices is dependent on the column ordering. Recall that the FARO loss is the minimum generalized Hamming distance between all column permutations of two feature allocation matrices. Under the left-ordering equivalence class, the ordering of the columns should not matter — any reordering of the columns of a binary feature allocation matrix are equivalent. As in Ni et al. (2020b), we would like to remove this dependency by optimally reordering or aligning the columns (features) of two binary matrices Z, \hat{Z} such that the distance is minimized. Their method computes and compares all possible column orderings of each Z in order to find this minimizing alignment, which was feasible in their study because the matrices of interest usually contained six or fewer features. However, for a case where $K = 10$, there would be $10! \approx 3.63 \times 10^6$ possible alignments (see Table 1). Clearly, carrying out this many evaluations of the distance between a candidate and many posterior samples would be computationally prohibitive.

One of the key contributions of this paper is recognizing that the optimal alignment task is a linear assignment problem, for which fast algorithms are available. Rapid computation of the optimal alignment permits repeated computation of FARO loss, which enables our FANGS method (Section 4) to be feasible for feature allocation estimation. The linear

assignment problem (in its balanced form) is often described in the context of agents and tasks; each of K agents can be assigned to one and only one of K tasks. A small example is illustrated in Figure 2 and Equation 7. In our case, the “agents” are the K features from Z and the “tasks” are the K features from \hat{Z} . There is a cost for assigning a particular agent to a particular task; in our case, this represents the fact that there is some generalized Hamming distance between a particular column of Z and a particular column of \hat{Z} . The end goal is to assign each agent to a task such that the sum of the costs is minimized, while avoiding an exhaustive search of all possible alignments.

The linear assignment problem avoids an exhaustive search of all alignments because it is essentially a constrained minimization problem. The objective function is the trace of a transposed permutation matrix \mathbf{X} multiplied by a cost matrix $\mathbf{C}(Z, \hat{Z})$. The $K \times K$ cost matrix is constructed such that $\mathbf{C}_{ij}(Z, \hat{Z})$ represents the cost (or generalized Hamming distance) of lining up feature i of Z with feature j of \hat{Z} . The constraints of the minimization problem follow directly from the definition of the permutation matrix: \mathbf{X} is a $K \times K$ binary matrix having exactly one nonzero entry in each row and column (Brualdi, 2006). In other words, we must choose exactly one item in each row and column in order to define a valid alignment of the matrices such that the total cost (total generalized Hamming distance) is minimized. In the simple example in Figure 2 and Equation 7, the minimizing alignment is $x_{12} = x_{23} = x_{31} = x_{44} = 1$, leading to a cost of $3 + 2 + 4 + 2 = 11$. For our purposes, this implies that column 1 of Z should be aligned with column 2 of \hat{Z} , column 2 of Z with column 3 of \hat{Z} , and so forth, such that the FARO loss is 11.

$$\begin{aligned}
 \mathbf{X} &= \begin{bmatrix} x_{11} & x_{12} & x_{13} & x_{14} \\ x_{21} & x_{22} & x_{23} & x_{24} \\ x_{31} & x_{32} & x_{33} & x_{34} \\ x_{41} & x_{42} & x_{43} & x_{44} \end{bmatrix} & \mathbf{C}(Z, \hat{Z}) &= \begin{bmatrix} 14 & 3 & 5 & 8 \\ 5 & 12 & 2 & 6 \\ 4 & 7 & 7 & 10 \\ 9 & 2 & 5 & 2 \end{bmatrix} & \text{Objective Function:} \\
 & & & & f(Z, \hat{Z}) &= \text{tr}(\mathbf{X}' \mathbf{C}(Z, \hat{Z})) \\
 \text{Constraints:} & \sum_{i=1}^4 x_{ij} = \sum_{j=1}^4 x_{ij} = 1 \text{ and } x_{ij} \in \{0, 1\}; i, j \in \{1, \dots, 4\} & & & & (7)
 \end{aligned}$$

The linear assignment problem is quickly solved by the Jönker and Volgenant (1987) algorithm in the computer science literature, which builds on an earlier solution called the Hungarian algorithm. Their algorithm is guaranteed to return an optimal alignment

K	Traditional Approach (All Permutations)		Our Approach (Linear Assignment)	
	$K!$	Time (ms)	K^3	Time (ms)
4	24	0.04	64	0.02
6	720	0.83	216	0.02
8	40,320	58.12	512	0.03
10	3,628,800	6,444.61	1,000	0.05

Table 1: Mean time (over 100 replications, in milliseconds) to find the minimum Hamming distance between two randomly sampled matrices with $n = 100$ rows and $K \in \{4, 6, 8, 10\}$ columns using (left) all possible permutations and (right) the Jönker-Volgenant algorithm. Note that it took more than 6 seconds to examine all permutations for $K = 10$, whereas the Jönker-Volgenant algorithm only took a fraction of a millisecond.

and does so much faster than an exhaustive search. For our software implementation of the FARO loss, we use an implementation of the Jönker-Volgenant algorithm provided in the Rust crate `lapjv` (Dmytrenko, 2021), which has $\mathcal{O}(K^3)$ complexity. Recall that the distance computation for feature allocations from Ni et al. (2020b) examined all column permutations of each matrix making it viable only for small values of K because it has order $\mathcal{O}(K!)$. A rapidly computed loss function, especially when K is large, is critical in order to successfully implement a more thorough search algorithm. Table 1 shows the mean time to compute the minimum Hamming distance for both approaches. Spending even 6 seconds to compute the loss between two feature allocations with $K = 10$ features using an exhaustive search may be too much for a robust optimization procedure, but the Jönker-Volgenant algorithm makes this trivial even for large K .

3.5 Quasi-Metric Properties of FARO Loss

A metric satisfies three properties: 1) the identity of indiscernibles, 2) symmetry, and 3) the triangle inequality. A quasi-metric is a function that satisfies the identity of indiscernibles and triangle inequality but does not need to satisfy the symmetry property. In this section we prove that FARO loss is a quasi-metric when $a \neq b$ and a metric when $a = b = 1$. We also discuss why each property is desirable for a feature allocation loss function.

Theorem 1. *FARO loss is a quasi-metric on the feature allocation space.*

Before proceeding with the proof, it is helpful to point out that Hamming distance (under the equal penalty assumption) has already been proven to be a metric by [Robinson \(2003\)](#). It follows naturally that generalized Hamming distance satisfies the properties of a quasi-metric, which we prove in the appendix. Given that the generalized Hamming distance is a quasi-metric, we seek to prove that the minimum of $m = K!$ generalized Hamming distances is also a quasi-metric (where K is the number of columns in each feature allocation matrix after augmentation). To do this, we denote the FARO loss between two binary feature allocation matrices Z, \hat{Z} as follows, where each L_i is simply the generalized Hamming distance between Z and a distinct permutation of the columns of \hat{Z} .

$$L(Z, \hat{Z}) = \min\{L_1(Z, \hat{Z}), L_2(Z, \hat{Z}), \dots, L_m(Z, \hat{Z})\}.$$

A loss function L satisfies the identity of indiscernibles when $L(Z, \hat{Z}) = 0$ if and only if $Z = \hat{Z}$. First, suppose $L(Z, \hat{Z}) = 0$. Then there exists a loss function L_i among the m quasi-metrics that satisfies $L_i(Z, \hat{Z}) = 0$. Since each L_i is a quasi-metric and satisfies the identity of indiscernibles, it follows that $Z = \hat{Z}$. Conversely, suppose $Z = \hat{Z}$. Then for at least one quasi-metric $L_i \in \{L_1, L_2, \dots, L_m\}$, we have $L_i(Z, \hat{Z}) = 0$. Because at least one L_i is equal to zero, we have that $\min\{L_1(Z, \hat{Z}), L_2(Z, \hat{Z}), \dots, L_m(Z, \hat{Z})\} = 0$ so $L(Z, \hat{Z}) = 0$. Therefore $L(Z, \hat{Z}) = 0 \iff Z = \hat{Z}$, so FARO loss satisfies the identity of indiscernibles. A loss function with this property conforms closely to our intuition of distance, since two distinct feature allocations should have nonzero distance between them (and *vice versa*).

The triangle inequality requires that, for any three feature allocations Z_1, Z_2, Z_3 in the space of all possible feature allocations, $L(Z_1, Z_2) + L(Z_2, Z_3) \geq L(Z_1, Z_3)$. The triangle inequality establishes that if two feature allocations are similar to a third one, then those two feature allocations should also be similar to each other ([Dahl et al., 2022](#)). It also allows us to place an upper bound on the distance between two feature allocations if we know the distance from both of those feature allocations to another, meaning there is an intuitive structure to the space. In proving the triangle inequality for FARO loss, the following theorem (proven in the appendix) is useful.

Theorem 2. *The maximum of a finite set of functions that obey the triangle inequality*

also obeys the triangle inequality.

We will use Theorem 2 to prove the triangle inequality for FARO loss. Recall the characterization of FARO loss $L(Z, \hat{Z}) = \min\{L_1(Z, \hat{Z}), L_2(Z, \hat{Z}), \dots, L_m(Z, \hat{Z})\}$. Now, consider the function:

$$L^*(Z, \hat{Z}) = \max\{L_1(Z, 1 - \hat{Z}), L_2(Z, 1 - \hat{Z}), \dots, L_m(Z, 1 - \hat{Z})\},$$

where L^* is a related function to FARO loss using the same generalized Hamming distance metrics L_1, L_2, \dots, L_m , except now the *maximum* of these values is selected, and the second argument in each loss function is $1 - \hat{Z}$ (i.e., a matrix where each element of \hat{Z} is “flipped” from a 1 to a 0 and *vice versa*). By Theorem 2 we have that L^* satisfies the triangle inequality. Further, the maximizer of L^* corresponds to the minimizer of the FARO loss L (proven in the appendix). Therefore, the triangle inequality holds for FARO loss.

We conclude that FARO loss induces a quasi-metric space on feature allocations which behaves according to intuition for a distance function, with the exception of symmetry. However, our software maintains a standardized direction of computation such that asymmetry should not be a concern for users; they need only specify the value of a . When $a = b$, the symmetry property also holds, so in this special case, FARO loss is a metric and not just a quasi-metric (proven in appendix).

4 FANGS Algorithm

Having established a loss function that can easily compute the distance between feature allocations, we proceed to explain our novel search algorithm and how it builds on the FARO loss function. We call our search algorithm FANGS, an acronym for **f**eature **a**llocation **n**eighborhood-based **g**reedy **s**earch.

4.1 Algorithmic Description

The FANGS algorithm takes a list of posterior feature allocation samples as its main input, plus several tuning parameters. We introduce our description of this search algorithm with

Algorithm 1 Pseudocode for the FANGS algorithm. Let Z_1, \dots, Z_B be samples from the feature allocation distribution of interest. Let N_{iter} be the number of iterations, K_{max} be the maximum number of features present among the samples, N_{init} be the number of baseline samples used to obtain initial estimates, and N_{sweet} be the number of initial estimates used as starting points for the “sweetening phase” (i.e., optimization).

```

1:                                     ▷ Initialization phase
2: Augment samples with columns of zeros such that each has exactly  $K_{\text{max}}$  features.
3: for  $i$  in  $1, \dots, N_{\text{init}}$  do
4:   Let  $Z^{(i)}$  be randomly sampled without replacement from  $Z_1, \dots, Z_B$ .
5:   Align the columns of the remaining  $B - 1$  samples to  $Z^{(i)}$  to minimize Hamming distance.
6:   Compute the element-wise means (proportions of ones) across the  $B$  aligned samples.
7:   Form  $Z_i^*$  by thresholding all proportions (to 0 or 1) given the cutoff  $a/2$ .
8:   Remove any all-zero columns from  $Z_i^*$ .
9:   Calculate the expected FARO loss of  $Z_i^*$ .
10: Let  $\zeta_1, \dots, \zeta_{N_{\text{sweet}}}$  be the  $Z^*$ 's with the smallest expected FARO loss.
11:                                     ▷ Sweetening phase
12: for  $i$  in  $1, \dots, N_{\text{iter}}$  do
13:   for  $j$  in  $1, \dots, N_{\text{sweet}}$  do
14:     Propose  $\zeta_j^*$  by flipping a randomly selected entry of  $\zeta_j$  from 0 to 1 or vice versa.
15:     if the expected FARO loss of  $\zeta_j^*$  is less than that of  $\zeta_j$  then
16:       Set  $\zeta_j$  to  $\zeta_j^*$ .
17:     else
18:       Leave  $\zeta_j$  unchanged.
19: return the feature allocation with the smallest expected FARO loss among  $\zeta_1, \dots, \zeta_{N_{\text{sweet}}}$ .

```

pseudocode (in Algorithm 1) and then outline the purpose of each parameter. The search algorithm is implemented in the `fangs` package in R.

FANGS is comprised of two stages: an initialization phase and a sweetening phase. In the initialization phase, N_{init} feature allocations are randomly selected from the B samples. We refer to these N_{init} feature allocations as baselines. For each baseline, the B samples are realigned by column to minimize their generalized Hamming distance to the baseline. This is similar to the approach in Zeng et al. (2018), but our approach allows the incorporation of differential Hamming distance penalties and is much faster due to recognition of the linear assignment problem. This baseline alignment approach is also different from their alignment approach which aligned samples to each other sequentially, one after another, and is thus not parallelizable. For each set of B realigned samples, the element-wise mean is calculated, yielding an $n \times K_{\text{max}}$ matrix of proportions. Each proportions matrix is then thresholded to 0 or 1 using a cutoff point of $a/2 \in (0, 1)$. Lower values of a result in more

dense initial estimates (i.e., more values are thresholded to 1) and higher a leads to the opposite. This concept is further discussed and verified in Section 5.3. The result of the initialization phase is N_{init} initial feature allocation estimates.

From these initial estimates, only the N_{sweet} feature allocations with the lowest expected FARO losses are advanced to the sweetening phase. During the sweetening phase, the algorithm iterates through each of the N_{sweet} samples N_{iter} times. At each iteration, a randomly selected element of the binary matrix is “flipped” (i.e., switched from 0 to 1 or 1 to 0) and the algorithm checks to see if the flip lowered the expected loss. If so, the change is accepted and the old state is discarded; otherwise, the matrix remains unchanged. After sweetening each of the N_{sweet} matrices N_{iter} times, the feature allocation having the lowest (Monte Carlo estimate of the) expected FARO loss is returned as the point estimate.

4.2 Discussion of Parameters

For most of the search’s tuning parameters, there are versatile default values that are sufficient for the vast majority of applications. The N_{iter} argument is an influential parameter in terms of both loss minimization and wall time. Raising the number of iterations tends to lead to estimates with lower expected loss but also increases the computation time. The first set of samples in Figure 3 was smaller in dimension ($n = 20, K = 3$), so it did not take many iterations to stabilize to an estimate. The second set was larger ($n = 62, K = 77$) and continued to slowly find a better estimate given more iterations. We suggest $N_{\text{iter}} = 1000$ as the default value, which seems to provide a balance between computation time and loss minimization for a moderate number of samples and moderate matrix dimensions. However, for any particular dataset and application, we suggest considering other values for N_{iter} to balance stability of the estimate and time.

The default values for N_{init} and N_{sweet} are 16 and 4, respectively. These choices arise from the fact that both phases of FANGS (the initialization and the sweetening) can be run in parallel. It is now common for most systems, even personal desktops and laptops, to have 4 or more cores available. Thus, it seems logical to allow a default of 4 initial estimates and 4 sweetenings. However, the baseline alignment is much faster than the sweetening,

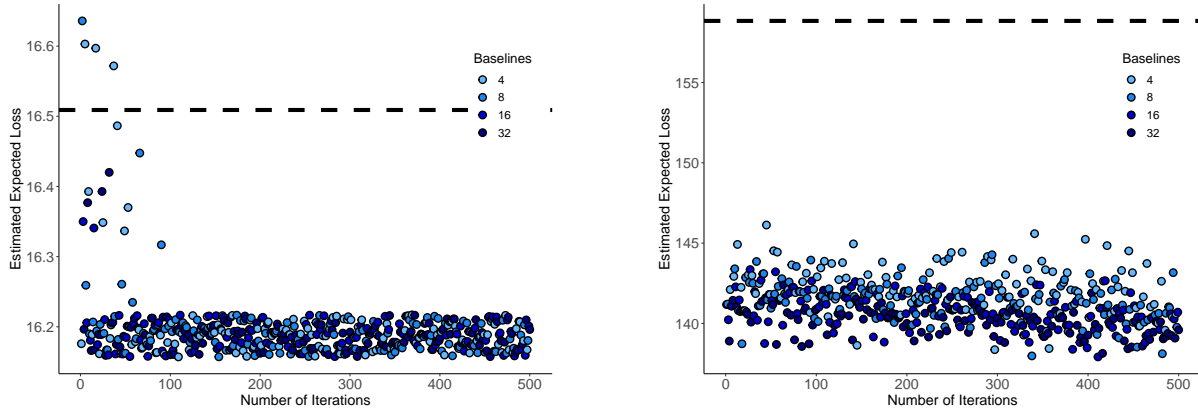


Figure 3: Jittered scatter plots displaying the estimated expected loss as a function of N_{iter} for two sets of samples from Warr et al. (2021). The dashed line indicates the estimated expected loss from the minimizing draw.

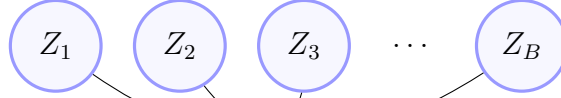
and we found it helpful to use more baselines when possible. With these parameters in mind, we offer Figure 4 as an illustration of FANGS under its default values.

4.3 Computational Complexity

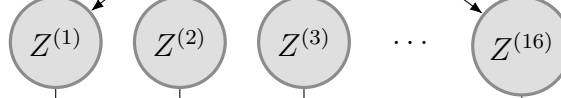
We already established the computational complexity for our FARO loss computation, derived from the Jönker-Volgenant Algorithm and implemented in Rust (Dmytrenko, 2021), to be $\mathcal{O}(K^3)$ for comparing feature allocations having up to K columns. To examine the computational burden of FANGS as a whole, we frame this $\mathcal{O}(K^3)$ complexity in the context of repeatedly scoring the expected loss for many feature allocations among a set of B posterior samples.

To obtain N_{init} sets of realigned samples, FARO loss is computed $B N_{\text{init}}$ times, yielding a complexity of $\mathcal{O}(K^3 B N_{\text{init}})$. Then, the expected loss for each of the N_{init} initial estimates is computed, which also has complexity $\mathcal{O}(K^3 B N_{\text{init}})$. Adding these components and simplifying yields $\mathcal{O}(K^3 B N_{\text{init}} + K^3 B N_{\text{init}}) \equiv \mathcal{O}(2K^3 B N_{\text{init}}) \equiv \mathcal{O}(K^3 B N_{\text{init}})$ in the initialization phase. In the sweetening phase, the expected FARO loss is estimated once per iteration in each sweetening. Thus, the order of the sweetening phase is $\mathcal{O}(K^3 B N_{\text{iter}} N_{\text{sweet}})$. These two phases are additive in FANGS, so the order of the search as a whole is $\mathcal{O}(K^3 B N_{\text{init}} + K^3 B N_{\text{iter}} N_{\text{sweet}})$, or equivalently, $\mathcal{O}\left((K^3 B) (N_{\text{init}} + N_{\text{iter}} N_{\text{sweet}})\right)$. Although this may seem convoluted, the key takeaway is that the number of features K is

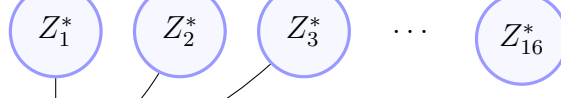
A) Randomly select 16 baselines from the B samples:



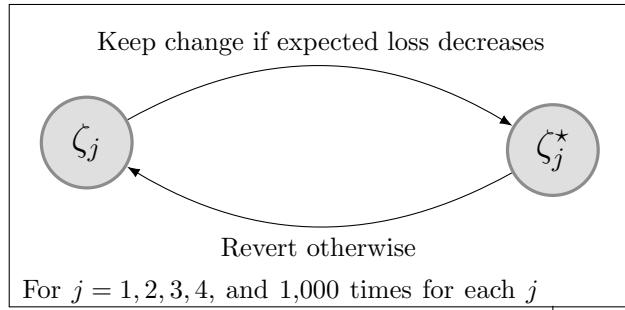
B) Align all B samples to each baseline, compute proportions, and threshold:



C) Score the expected loss for each initial estimate and keep the 4 best for sweetening:



D) Randomly flip entries 1,000 times for each sweetening:



E) Final estimate ζ is the ζ_j^* with the lowest expected loss.



Figure 4: FANGS algorithm overview using default settings.

the most influential in adding to or lightening the computational expense of FANGS since it has the highest degree at 3. K may be slightly different for each matrix comparison since the number of features varies across draws, but if this variance is low, then the order could still be approximated as above using $K = \hat{K}$, the modal number of features from the samples.

5 Verifications

In this section, we compare the FANGS estimate to the minimizing draw for five different sets of posterior feature allocation samples obtained from previous studies.

Case Study	Observations (n)	Features (K)	Samples (B)
DFA (Ni et al., 2020b)	300	4	500
CMC (Ni et al., 2020a)	800	5	500
SIFA (Zeng et al., 2018)	80	6	4000
AIBD (Warr et al., 2021)	20	3	1000
Alzheimer’s (Warr et al., 2021)	62	77	3000

Table 2: Values of n and K for the true feature allocation matrix Z that was used to generate B samples in the simulations for each case study. The Alzheimer’s samples were based on real data, so 77 represents \hat{K} instead of the “true K ”.

5.1 Description of Posterior Samples

Of the five sets of posterior feature allocation samples examined, two of them are from Warr et al. (2021) and were already used in Section 4 (a smaller set simulated directly from their linear latent feature model and a larger set from real Alzheimer’s disease data). In addition, we have samples from the CMC study (Ni et al., 2020a), the SIFA study (Zeng et al., 2018), and scenario 1 of the DFA model (Ni et al., 2020b)². These papers were discussed previously and their posterior samples are summarized in Table 2.

5.2 Simulation Study

It only makes sense to compare search algorithms if the loss function is held constant across all searches. Having already outlined why FARO loss holds practical advantages over the others, we fix FARO loss as the loss function for all case studies and compare the FANGS estimate against the loss-minimizing draw. The simulations were run on a server with 512 GB of RAM and two Intel Xeon Gold 6142 CPU @ 2.60GHz processor, yielding 32 physical cores and 64 cpu threads. Although FANGS is a stochastic algorithm, the use of 16 baselines and 1,000 iterations resulted in almost no noticeable stochasticity. Table 3 shows the estimated expected loss and wall time under each estimate and case study. Not only does FANGS find estimates with lower expected loss than the minimizing draw, but it appears to do so in a shorter window of time when K is higher. FANGS takes longer for

²In the DFA study, Z followed a complex structure with 6 features. Some information in the first two features was treated as fixed, so we ignore these first two features and assume $K = 4$.

Study	Draws Method		FANGS	
	Exp. Loss	Runtime	Exp. Loss	Runtime
DFA	17.51	0.14	14.78	0.36
CMC	103.35	0.70	102.21	0.72
SIFA	50.45	3.77	43.48	1.83
AIBD	16.51	0.21	16.19	0.70
Alzheimer’s	158.84	151.18	138.94	32.06

Table 3: The expected loss from the minimizing draw and from the FANGS estimate (using default parameters), as well as the corresponding wall times (in seconds) averaged over 1000 replications for each case study. Monte Carlo error was nonexistent for the first four case studies and negligible for the Alzheimer’s samples.

the AIBD and DFA studies, is about the same for the CMC study, and is much faster for the SIFA and Alzheimer’s samples.

In short, FANGS reliably produces a feature allocation estimate with significantly lower expected loss than the draws estimate in a comparable window time (if not more quickly) using default parameters. FARO loss and FANGS are implemented in R with a fast and easy-to-use software package. FANGS could also be applied to other loss functions should others be developed in the future. It is critical, however, that any new loss function be able to be rapidly and repeatedly evaluated, otherwise it may not be viable in a search algorithm like FANGS.

5.3 Differential Penalties

In Section 3.3, we introduced generalized Hamming distance and discussed using $a \neq b$ to assign lower FARO loss to more dense or sparse feature allocations. As a test case, we examine the Alzheimer’s samples from the AIBD study ($n = 62$), which had samples ranging from $K = 5$ to $K = 94$. Figure 5 shows that the feature allocation estimate is more dense when a is lower (closer to 0) and more sparse as a approaches 2. Even when K didn’t change by as much between increments of a (i.e. $a = 0.1$ and $a = 0.5$), the sparsity of the individual features still did (from 790 to 446 total entries in that instance). Furthermore, the largest decreases in K (for the estimates) correspond to the highest-density region of the distribution of K in the original samples. Similar trends were present for the other sets

a	b	K	Entries
0.01	1.99	85	1722
0.1	1.9	81	790
0.5	1.5	79	446
1.0	1.0	74	338
1.5	0.5	60	242
1.9	0.1	27	112
1.99	0.01	6	14

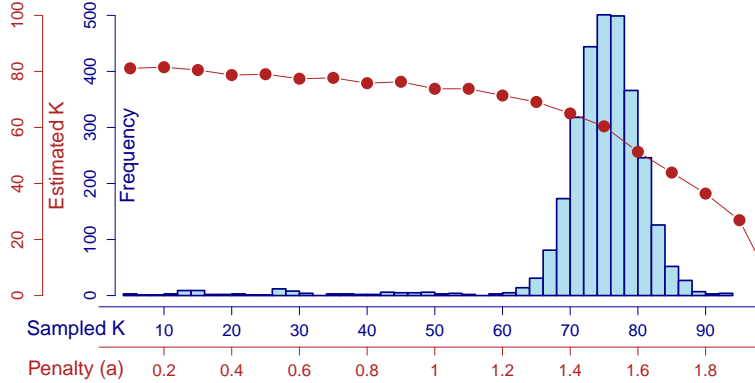


Figure 5: Total number of features K and entries in the FANGS estimate from the Alzheimer’s samples for $a \in (0, 2)$, overlaid with the distribution of K in the original samples.

of samples, although it is more prominent here due to the high variance of K . We conclude that the incorporation of differential penalties in FARO loss (and by extension, FANGS) successfully allows for sparsity tuning in the feature allocation estimation process.

6 Conclusion

Previous feature allocation studies typically developed their own loss function tailored directly to the estimation problem at hand, then performed minimization over the posterior samples. FARO loss is more broadly applicable, accommodates feature allocations with different numbers of features, and does not depend on the feature ordering. It satisfies the properties of a quasi-metric and is computed quickly using optimization techniques from the linear assignment problem. Because the loss is so rapidly evaluated, FANGS is able to better explore the feature allocation space than the draws method. In the case studies we examined, FANGS consistently found an estimate with lower expected loss than any of the posterior samples. We believe that FARO loss and FANGS are effective and versatile enough to serve as a general loss function and search algorithm for feature allocation estimation problems.

7 Appendix

Theorem 2. *The maximum of a finite set of functions that obey the triangle inequality also obeys the triangle inequality.*

Proof: Let X be a set of all feature allocations for n items and let d_1, \dots, d_m be real-valued functions defined on $X \times X$ which obey the triangle inequality. Without loss of generality, we first seek to show that the maximum of d_1 and d_2 obeys the triangle inequality. For all $x, y \in X$, let $d_{1,2}(x, y) = \max\{d_1(x, y), d_2(x, y)\}$. We must show that, for any $x, y, z \in X$, $d_{1,2}(x, y) + d_{1,2}(y, z) \geq d_{1,2}(x, z)$. Recall that, since both d_1 and d_2 obey the triangle inequality, $d_1(x, y) + d_1(y, z) \geq d_1(x, z)$ and $d_2(x, y) + d_2(y, z) \geq d_2(x, z)$. But, by the definition of $d_{1,2}$, the left-hand-side of each of these inequalities is less than or equal to $d_{1,2}(x, y) + d_{1,2}(y, z)$. Then, $d_{1,2}(x, y) + d_{1,2}(y, z)$ is greater or equal to both $d_1(x, z)$ and $d_2(x, z)$ and, therefore, greater than or equal to $\max\{d_1(x, z), d_2(x, z)\} = d_{1,2}(x, z)$. Therefore $d_{1,2}$ obeys the triangle inequality.

We can again apply this result to get that $d_{1,2,3}(x, y) = \max\{d_{1,2}(x, y), d_3(x, y)\} = \max\{\max\{d_1(x, y), d_2(x, y)\}, d_3(x, y)\} = \max\{d_1(x, y), d_2(x, y), d_3(x, y)\}$ also obeys the triangle inequality. Repeatedly applying this result for all integers until m yields:

$$d_{1,\dots,m}(x, y) = \max\{d_{1,\dots,m-1}(x, y), d_m(x, y)\} = \max\{d_1(x, y), \dots, d_m(x, y)\}$$

Hence, $d_{1,\dots,m}(x, y)$ obeys the triangle inequality.

Theorem 3. *The generalized Hamming distance is a quasi-metric on the feature allocation space for any $a, b > 0$ where $a + b = 2$.*

For brevity, we denote $\mathbb{I}(Z_{ij} = 1)$ as \mathbb{Z}_{ij} and $\mathbb{I}(Z_{ij} = 0)$ as \mathbb{Z}_{-ij} for any binary feature allocation matrix Z . Also, let $\mathbb{I}(Z_{ij} = 1 \cap \hat{Z}_{ij} = 1) = \mathbb{Z}_{ij} \hat{\mathbb{Z}}_{ij}$.

Proof: Identity of Indiscernibles: Suppose $Z = \hat{Z}$. Then for all $1 < i < n, 1 < j < K$, we have that $\mathbb{Z}_{ij} \hat{\mathbb{Z}}_{-ij} = 0$ and $\mathbb{Z}_{-ij} \hat{\mathbb{Z}}_{ij} = 0$. Then, $\sum_{i=1}^n \sum_{j=1}^K [a(0) + b(0)] = 0$, so $L(Z, \hat{Z}) = 0$. We prove the converse using its contrapositive. Suppose $Z \neq \hat{Z}$; that is, there exists at least one pair of (i, j) such that $Z_{ij} \neq \hat{Z}_{ij}$. It follows that:

$$L(Z, \hat{Z}) = \sum_{i=1}^n \sum_{j=1}^K \left[a \mathbb{Z}_{ij} \hat{\mathbb{Z}}_{-ij} + b \mathbb{Z}_{-ij} \hat{\mathbb{Z}}_{ij} \right] \geq \min(a, b)$$

Since a and b are both positive real numbers, $\min(a, b) > 0$, and so $L(Z, \hat{Z}) > 0$.

Triangle Inequality: Given three feature allocations U, V, W defined on the same feature allocation space, the triangle inequality holds for generalized Hamming distance if $L(U, V) + L(V, W) - L(U, W) \geq 0$. The left side of this expression simplifies to:

$$a \cdot \sum_{i=1}^n \sum_{j=1}^K \left[\mathbb{U}_{ij} \mathbb{V}_{-ij} + \mathbb{V}_{ij} \mathbb{W}_{-ij} - \mathbb{U}_{ij} \mathbb{W}_{-ij} \right] + b \cdot \sum_{i=1}^n \sum_{j=1}^K \left[\mathbb{U}_{-ij} \mathbb{V}_{ij} + \mathbb{V}_{-ij} \mathbb{W}_{ij} - \mathbb{U}_{-ij} \mathbb{W}_{ij} \right]$$

We examine each of the two summations to see if either component can be less than zero for any (i, j) index. We can also disregard a and b for this purpose since they are both positive real values. The only way the first summation can be less than zero is if $\mathbb{U}_{ij} \mathbb{V}_{-ij}$ and $\mathbb{V}_{ij} \mathbb{W}_{-ij}$ are both false, while $\mathbb{U}_{ij} \mathbb{W}_{-ij}$ also holds true. For the first two indicators to both be false, we need one of the following conditions to hold:

$$(i) \mathbb{U}_{-ij} \mathbb{V}_{-ij} \mathbb{W}_{-ij} \quad (ii) \mathbb{U}_{ij} \mathbb{V}_{ij} \mathbb{W}_{ij} \quad (iii) \mathbb{U}_{-ij} \mathbb{V}_{ij} \mathbb{W}_{ij} \quad (iv) \mathbb{U}_{-ij} \mathbb{V}_{-ij} \mathbb{W}_{ij}$$

In any of the above cases, the indicator $\mathbb{U}_{ij} \mathbb{W}_{-ij}$ does not hold true, and so the first line of the expression would evaluate to zero. A nearly identical approach follows for the second summation with b . Finally, we conclude that $L(U, V) + L(V, W) - L(U, W) \geq 0$ because it is a sum of strictly nonnegative terms. Therefore $L(U, V) + L(V, W) \geq L(U, W)$, and the triangle inequality is met for generalized Hamming distance.

Lemma 1. *The maximizing column permutation of L^* corresponds to the minimizing permutation of FARO loss.*

Proof: The following proof holds regardless of whether a and b are equal or not. Recall the function L^* which was previously defined in Section 3 as:

$$L^*(Z, \hat{Z}) = \max\{L_1(Z, 1 - \hat{Z}), L_2(Z, 1 - \hat{Z}), \dots, L_m(Z, 1 - \hat{Z})\}, \text{ where } m = K!$$

Denote $L_i(Z, 1 - \hat{Z})$ as $L(Z, 1 - \hat{Z}^{(i)})$, where L is just the generalized Hamming distance function but now $\hat{Z}^{(i)}$ is the feature allocation matrix \hat{Z} with columns permuted according to the i th permutation, $i = 1, 2, \dots, m$. Then $L(Z, 1 - \hat{Z})$ is simplified as follows:

$$\sum_{\ell=1}^n \sum_{j=1}^K \left[a \mathbb{Z}_{\ell j} (1 - \hat{Z}^{(i)})_{-\ell j} + b \mathbb{Z}_{-\ell j} (1 - \hat{Z}^{(i)})_{\ell j} \right] = \sum_{\ell=1}^n \sum_{j=1}^K \left[a \mathbb{Z}_{\ell j} \hat{Z}_{\ell j}^{(i)} + b \mathbb{Z}_{-\ell j} \hat{Z}_{-\ell j}^{(i)} \right]$$

$$\begin{aligned}
&= nK(a + b) - \sum_{\ell=1}^n \sum_{j=1}^K [a \mathbb{Z}_{-\ell j} + b \mathbb{Z}_{\ell j}] - \left[a \cdot \sum_{\ell=1}^n \sum_{j=1}^K \mathbb{Z}_{\ell j} \hat{Z}_{-\ell j}^{(i)} + b \cdot \sum_{\ell=1}^n \sum_{j=1}^K \mathbb{Z}_{-\ell j} \hat{Z}_{\ell j}^{(i)} \right] \\
&= nK(a + b) - \sum_{\ell=1}^n \sum_{j=1}^K [a \mathbb{Z}_{-\ell j} + b \mathbb{Z}_{\ell j}] - L(Z, \hat{Z}^{(i)})
\end{aligned}$$

Note that the first two terms in the final line of the equality do not depend on the column ordering of Z or \hat{Z} , since the total numbers of ones or zeros in Z is the same no matter how its columns are arranged. Therefore, we have:

$$\arg \max_i \{L(Z, 1 - \hat{Z}^{(i)})\} = \arg \max_i \{-L(Z, \hat{Z}^{(i)})\} = \arg \min_i \{L(Z, \hat{Z}^{(i)})\}$$

We have now shown that the maximizing column permutation for L^* is the same as the minimizing column permutation for L , or FARO loss.

Lemma 2. *The symmetry property holds for FARO loss in the special case that $a = b = 1$.*

Proof: The notation from Section 3 is used. Note that when $a = b = 1$, L_1, L_2, \dots, L_m are all metrics, as the generalized Hamming distance in this special case reverts to the normal Hamming distance (which (Robinson, 2003) proved is a metric). A loss function L satisfies symmetry when $L(Z, \hat{Z}) = L(\hat{Z}, Z) \forall Z, \hat{Z}$. It is simple to see that $L(Z, \hat{Z}) = \min\{L_1(Z, \hat{Z}), L_2(Z, \hat{Z}), \dots, L_m(Z, \hat{Z})\} = \min\{L_1(\hat{Z}, Z), L_2(\hat{Z}, Z), \dots, L_m(\hat{Z}, Z)\}$ since L_1, L_2, \dots, L_m are all metrics. By definition of L , we have $\min\{L_1(\hat{Z}, Z), L_2(\hat{Z}, Z), \dots, L_m(\hat{Z}, Z)\} = L(\hat{Z}, Z)$. Thus $L(Z, \hat{Z}) = L(\hat{Z}, Z)$, so the symmetry property holds.

References

- Binder, D. A. (1978), “Bayesian cluster analysis,” *Biometrika*, 65, 31–38.
- Bookstein, A., Kulyukin, V., and Raita, T. (2002), “Generalized hamming distance,” *Information Retrieval*, 5, 353–375.
- Brualdi, R. A. (2006), *Combinatorial matrix classes*, Cambridge University Press.
- Dahl, D. B. (2006), “Model-Based Clustering for Expression Data via a Dirichlet Process

- Mixture Model,” in Do, K.-A., Müller, P., and Vannucci, M. (editors), *Bayesian Inference for Gene Expression and Proteomics*, Cambridge University Press, 201–218.
- Dahl, D. B., Johnson, D. J., and Müller, P. (2022), “Search Algorithms and Loss Functions for Bayesian Clustering,” *Journal of Computational and Graphical Statistics*, 0, 1–35.
- Dahl, D. B. and Newton, M. A. (2007), “Multiple hypothesis testing by clustering treatment effects,” *Journal of the American Statistical Association*, 102, 517–526.
- Dmytrenko, A. (2021), *Linear assignment problem solver using Jonker-Volgenant algorithm*, URL <https://crates.io/crates/lapjv>. Rust crate version 0.2.1.
- Gershman, S. J., Frazier, P. I., and Blei, D. M. (2015), “Distance dependent infinite latent feature models,” *IEEE Transactions on Pattern Analysis and Machine Intelligence*, 37, 334–345.
- Griffiths, T. L. and Ghahramani, Z. (2011), “The Indian Buffet Process: An introduction and review,” *J. Mach. Learn. Res.*, 12, 1185–1224.
- Jönker, R. and Volgenant, A. (1987), “A shortest augmenting path algorithm for dense and sparse linear assignment problems,” *Computing*, 38, 325–340.
- Lau, J. W. and Green, P. J. (2007), “Bayesian Model-Based Clustering Procedures,” *Journal of Computational and Graphical Statistics*, 16, 526–558.
- Lui, A., Lee, J., Thall, P. F., Daher, M., Rezvani, K., and Barar, R. (2021), “A Bayesian feature allocation model for identification of cell subpopulations using cytometry data,” *arXiv preprint arXiv:2002.08609*.
- Ni, Y., Ji, Y., and Müller, P. (2020a), “Consensus Monte Carlo for random subsets using shared anchors,” *Journal of Computational and Graphical Statistics*, 29, 703–714.
- Ni, Y., Müller, P., and Ji, Y. (2020b), “Bayesian double feature allocation for phenotyping with electronic health records,” *Journal of the American Statistical Association*, 115, 1620–1634.

- Robinson, D. J. (2003), *An Introduction to Abstract Algebra*, De Gruyter, Inc.
- Wade, S. and Ghahramani, Z. (2018), “Bayesian cluster analysis: point estimation and credible balls (with discussion),” *Bayesian Analysis*, 13, 559–626.
- Warr, R. L., Dahl, D. B., Meyer, J. M., and Lui, A. (2021), “The Attraction Indian Buffet Distribution,” *Bayesian Analysis*.
- Xu, Y., Müller, P., Yuan, Y., Gulukota, K., and Ji, Y. (2015), “MAD Bayes for tumor heterogeneity - feature allocation with exponential family sampling,” *Journal of the American Statistical Association*, 110, 503–514.
- Zeng, L., Warren, J., and Zhao, H. (2018), “Phylogeny-based tumor subclone identification using a Bayesian feature allocation model,” *The Annals of Applied Statistics*, 13.